Published in final edited form as:
Neuroscience. 2008 June 12; 154(1): 381–389. doi:10.1016/j.neuroscience.2008.02.032.

Rapid Regulation of Microtubule-Associated Proteins 2 (MAP2) in Dendrites of N. Laminaris of the Chick Following Deprivation of Afferent Activity

Yuan Wang and **Edwin W Rubel**
Virginia Merrill Bloedel Hearing Research Center, Department of Otolaryngology-Head and Neck Surgery, University of Washington School of Medicine, Box 357923, Seattle, WA 98195, USA

Abstract

Differential innervation of segregated dendritic domains in the chick nucleus laminaris (NL), composed of third-order auditory neurons, provides a unique model to study synaptic regulation of dendritic structure. Altering the synaptic input to one dendritic domain affects the structure and length of the manipulated dendrites while leaving the other set of unmanipulated dendrites largely unchanged. Little is known about the effects of neuronal input on the cytoskeletal structure of NL dendrites and whether changes in the cytoskeleton are responsible for dendritic remodeling following manipulations of synaptic inputs. In this study, we investigate changes in the immunoreactivity of high-molecular weight microtubule associated protein 2 (MAP2) in NL dendrites following two different manipulations of their afferent input. Unilateral cochlea removal eliminates excitatory synaptic input to the ventral dendrites of the contralateral NL and the dorsal dendrites of the ipsilateral NL. This manipulation produced a dramatic decrease in MAP2 immunoreactivity in the deafferented dendrites. This decrease was detected as early as three hours following the surgery, well before any degeneration of afferent axons. A similar decrease in MAP2 immunoreactivity in deafferented NL dendrites was detected following a midline transection that silences the excitatory synaptic input to the ventral dendrites on both sides of the brain. These changes were most distinct in the caudal portion of the nucleus where individual deafferented dendritic branches contained less immunoreactivity than intact dendrites. Our results suggest that the cytoskeletal protein MAP2, which is distributed in dendrites, perikarya, and postsynaptic densities, may play a role in deafferentation-induced dendritic remodeling.

Keywords

deafferentation; dendritic plasticity; afferent regulation; cytoskeleton

Microtubules are a major cytoskeletal component of neuronal dendritic structure. It is well established that microtubule associated protein 2 (MAP2) binding increases the stability of the microtubule network and dendritic structure (Serrano et al., 1984; Kowalski and Williams, 1993; Yamauchi et al., 1993; Sánchez et al., 2000; Harada et al., 2002). MAP2 has been proposed to play a fundamental role as a regulator of dendritic morphology in the developing

Correspondence to: Edwin W Rubel, Virginia Merrill Bloedel Hearing Research Center, University of Washington, Mail Stop 357923, Seattle, WA 98195, Phone: (206) 543-8360, Fax: (206) 616-1828, Email: E-mail: rubel@u.washington.edu.
Handling editor: Professor O.P. Ottersen

and adult brain. This idea is supported by dynamic regulation of MAP2 expression and its involvement in dynamic changes in neuronal morphology caused by excitotoxins (Siman and Noszek, 1988; Bigot et al., 1991; Felipo et al., 1993; Arias et al., 1997; Faddis et al., 1997; Hoskison and Shuttleworth, 2006; Hoskison et al., 2007), traumatic brain injury (Taft et al., 1992; Folkerts et al., 1998), or focal ischemia (Pettigrew et al., 1996; Schwab et al., 1998). In addition, manipulations of synaptic activity alter the immunoreactivity for MAP2 in dendrites (Hendry and Bhandari, 1992; Steward and Halpain, 1999; Vaillant et al., 2002), further suggesting that synaptic activity either directly or indirectly regulates MAP2 expression.

The nucleus laminaris (NL) composed of third-order auditory neurons in the avian brainstem, receives segregated binaural excitatory input from the two ears via the nucleus magnocellularis (NM). The neurons of NL act as coincidence detectors and play an essential role in binaural hearing (Carr and Konishi, 1988, 1990; Overholt et al., 1992; Joseph and Hyson, 1993). This nucleus is thought to be analogous to the medial superior olivary nucleus of mammals (Burger and Rubel, 2007). NL provides a useful model for studying afferent regulation of dendritic structure and molecular mechanisms underlying this regulation (Deitch and Rubel, 1984; Sorensen and Rubel, 2006). In chicks, differential innervation of the segregated dendritic domains of NL allows local manipulation of the excitatory inputs to one dendritic domain, while leaving the other dendritic domain of the same cells intact to serve as a control. Specifically, neurons in NL contain a dorsal and a ventral set of dendrites that are essentially symmetrical and receive excitatory inputs almost exclusively from either the ipsilateral or the contralateral cochlea via NM, respectively (Parks and Rubel, 1975; Rubel et al., 2004). Consequently, excitatory inputs to one set of NL dendrites can easily be silenced or altered by manipulating the ipsilateral or contralateral projection of NM neurons. Previous studies have demonstrated a rapid retraction of the ventral NL dendrites within hours after transection of the contralateral NM projection, while the dorsal NL dendrites, receiving intact input, appear largely unaffected (Benes et al., 1977; Deitch and Rubel, 1984; Sorensen and Rubel, 2006).

Little is known regarding the role of synaptic input on the cytoskeletal structure of NL dendrites and whether changes in the cytoskeleton are responsible for deafferentation-induced dendritic retraction. High-molecular weight MAP2s (HMWMAP2), including MAP2A and MAP2B, are of particular interest because of their direct association with microtubules in dendrites and perikarya, as well as colocalization with actin in dendritic spines and postsynaptic densities (see review, Sánchez et al., 2000). To determine whether dendritic HMWMAP2 of NL neurons has a possible role in structural changes after alterations of synaptic input, we examined changes in the immunoreactivity for HMWMAP2 in NL dendrites following two different manipulations of excitatory afferents from NM (Fig. 1). Our results demonstrate a rapid reduction of the immunoreactivity for HMWMAP2 in the dendrites with reduced excitatory drive compared to dendrites that received normal synaptic input.

Experimental procedures

White Leghorn chicken hatchlings (*Gallus domesticus*) of 4–11 days of age were used. All procedures were carried out in accordance with the National Institute of Health Guide for the Care and Use of Laboratory Animals and approved by the University of Washington Institutional Animal Care and Use Committee.

Transection of the crossed dorsal cochlear tract (XDCT)

Animals were anesthetized with a mixture of 40 mg/kg ketamine and 12 mg/kg xylazine. The animals were placed in a head holder and surgery was conducted using the method of Deitch and Rubel (1984). Briefly, the neck muscles were resected to expose the dura covering the cerebellomedullary cistern. An ophthalmic knife was inserted through the dura and the fourth ventricle and into the brain stem so as to transect the XDCT at the midline. The wound was

packed with gelfoam and sealed with a tissue adhesive, LiquiVet (Oasis Medical, Mettawa, IL). The location and extent of the transection was examined after further tissue processing (see below). Only animals receiving a complete transection of the XDCT were used for data analysis.

Unilateral cochlea removal

The procedure described in Born and Rubel (1985) was used. Animals were anesthetized as described above. A small incision was made to widen the external auditory meatus of the right ear. The tympanic membrane and columella were removed to expose the oval window. The basilar papilla, including the lagena macula, was removed via the oval window using fine forceps, floated on water, and examined with a surgical microscope to verify complete removal. Only animals with a complete removal of the basilar papilla, including the lagena, were used for further tissue processing and data analysis. The incision was sealed with LiquiVet adhesive.

Immunohistochemistry

After survival times of 1, 3, 6, 14 hours, or 1 week (for cochlea removal only), the animals were transcardially perfused with 0.9% saline followed by 4% paraformaldehyde in 0.1 M phosphate buffer (PB; pH 7.4). The brains were removed from the skull, postfixed overnight in the same fixative, and then transferred to 30% sucrose in 0.1 M phosphatebuffered saline (PBS; pH 7.4) until they sank. Completeness of the XDCT transection was verified under a microscope after removal of the cerebellum and incomplete cases were discarded. The brain was frozen, cut coronally at 30 μm on a freezing sliding microtome, and each section was collected in PBS. Alternate serial sections were stained for Nissl substance or immunocytochemically for MAP2 using peroxidase or fluorescent immunocytochemical methods. Briefly, free-floating sections were incubated with primary antibody solutions diluted 1:1000 in PBS with 0.3% Triton X-100 overnight at 4°C, followed by biotinylated anti-IgG antibodies (1:200; Vector Laboratories, Burlingame, CA) or AlexaFluor® secondary antibodies (1:200; Molecular Probes, Eugene, OR) for 1–2 hours at room temperature. Monoclonal anti-MAP2 (cat. #MAB3418) made in mouse was purchased from Chemicon International (Temecula, CA). The immunogen is Bovine brain microtubule protein. The antibody binds specifically to MAP2a and MAP2b and is detected as a 300 kD band in western blot analysis.

For peroxidase immunocytochemical staining, sections were then incubated in avidin-biotin-peroxidase complex solution (ABC Elite kit; Vector Laboratories) diluted 1:100 in PBS with 0.3% Triton X-100 for 1 hour at room temperature. Sections were incubated for 3–5 minutes in 0.045% 3-3 -diaminobenzidine (Sigma, St. Louis, MO) with 0.03% hydrogen peroxide, 125 mM sodium acetate, 10 mM imidazole, and 100 mM nickel ammonium sulfate. Sections were mounted on gelatin-coated slides and then dehydrated, cleared, and coverslipped with DPX mounting medium (EMS, Hatfield, PA). For fluorescent immunocytochemical staining, sections were mounted and coverslipped with Fluoromount-G® (SouthernBiotech, Birmingham, AL).

Data analysis

Relative changes between the deafferented and intact dendrites of NL in MAP2 immunoreactivity following cochlea removal were quantified by comparing average optical densities of the immunostaining between the dorsal and ventral NL dendritic domains. Between two and five cases of each survival time group were chosen for this analysis. For each case, sections with fluorescent immunocytochemical staining were taken from the caudal and rostral portions of NL at the levels comparable to those of Figure 2A and 2C, respectively. A photomicrograph of NL was taken using a 20X objective at a total magnification of 240X (see Fig. 3). Although the dorsal and ventral dendrites of each NL cell are normally of equivalent

size (Smith and Rubel, 1979; Smith, 1981), the width of the dendritic regions will vary between the dorsal and ventral regions in individual sections due to slightly different slicing planes across cases. A box covering the major dendritic MAP2 staining was drawn first in the dendritic domain with a narrower width. Then the exact same size box was applied to the complementary domain. Average optical density of the box in the dorsal and ventral NL was measured using Image J software (version 1.38X; National Institutes of Health).

We defined D and V as the average density of staining in the dorsal and ventral neuropil domains, respectively. The Percent Difference was calculated as the change in density of the deafferented neuropil domain relative to the intact domain, which is (V-D) / D × 100 for the contralateral side and (D-V) / V ×100 for the ipsilateral side following cochlea removal. The percent difference was calculated within the same photomicrograph from the same section to avoid any possible inconsistencies caused by variations in immunostaining between cases and sections and variations in brightness across photos. The percent differences from all animals of the same group were averaged and plotted as a function of survival time. All statistical comparisons used the Prism ver. 4 software package (GraphPad Software, Inc., San Diego CA).

Results

MAP2 immunoreactivity in normal NL

In the chick, NL neurons are arranged in a single layer, except for the most caudolateral region of the nucleus where multiple layers of neurons are present. Dendrites of bipolar NL neurons are segregated into dorsal and ventral domains. Immunocytochemistry revealed a dense distribution of MAP2 in the dendrites and neuronal cell bodies whereas the immunoreactivity was absent in the nucleus. Figure 2 illustrates a series of coronal sections across NL. MAP2-immunoreactive dendrites are longer in the caudal and lateral portion of the nucleus than those located more rostrally and medially, reflecting the gradient of dendritic length in NL (Smith and Rubel, 1979;Smith, 1981;Deitch and Rubel, 1984). For sections with fluorescent immunocytochemical staining, the staining intensity is generally higher in the caudolateral NL than the rostromedial NL. Sections that were stained with peroxidase and intensified with nickel ammonium sulfate (see Experimental procedures) exhibited a more uniform staining intensity across the nucleus. However, at any particular location, the density of MAP2 immunostaining in individual dendritic branches appeared similar between the dorsal and ventral dendrites (Fig. 2 and 3A–B).

MAP2 immunoreactivity in NL following elimination of afferent action potential activity

Two methods were used to surgically eliminate the excitatory action potentials to one set of NL dendrites: unilateral cochlea removal and transection of the crossed dorsal cochlear tract (XDCT). The eighth nerve is the only excitatory input to NM neurons. Unilateral cochlea removal silences all the excitatory inputs to the ipsilateral NM and in turn to the dorsal dendrites of the ipsilateral NL and the ventral dendrites of the contralateral NL (Fig. 1A; Born et al., 1991). The XDCT contains the decussating NM axons that project to the ventral NL dendrites on both sides of the brain. A complete transection of XDCT at the midline eliminates all the excitatory inputs to the ventral dendrites of NL neurons, while leaving the inputs to the dorsal dendrites intact (Fig. 1B). After cochlea removal the cochlear ganglion cells and NM neurons begin to die about 18–24 hours after the surgery and by 24 hours about 30% NM neurons have degenerated (Rubel et al., 1990). After XDCT transection, the afferent terminals from NM on the ventral NL dendrites do not show any atrophic changes for at least the first 4 hours, and then they begin to degenerate (Deitch and Rubel, 1989). Fourteen animals received unilateral cochlea removal, 3 survived 1h, 2 survived 3h, 5 survived 6h, 2 survived 14h, and 2 survived

one week. Eight animals received a complete transection of XDCT, 3 survived 1h, 2 survived 3h, 2 survived 6h, and 1 survived 14h.

Changes in the pattern and intensity of MAP2 immunostaining following either manipulation were positively correlated with post-surgery survival time and varied with the location within the nucleus. At one hour of cochlea removal, the pattern and average density of MAP2 staining showed no discernable differences between the dorsal and ventral dendrites in any section of the nucleus, on both sides of the brain. Notable differences between MAP2 staining in the two dendritic domains were observed beginning at three hours post-surgery in the caudal portion of the nucleus and were detectable up to one week following deafferentation, the longest survival time examined. Low- and high-magnification photomicrographs in Figures 3 and 4 illustrate the MAP2 immunoreactivity in the caudal NL in a control and an experimental case that survived 14 hours following cochlea removal. In contrast to the similar staining intensity between the dorsal and ventral dendrites in the control (Fig. 3A–B), the deafferented dorsal dendrites of the ipsilateral NL and the ventral dendrites of the contralateral NL exhibited a lower density of staining than the complementary dendritic domain on the same side of the brain (Fig. 3C, 3E, 4A, and 4C). Corresponding spectrum images demonstrated that the deafferented dendritic domains contained fewer dendritic branches with high levels of staining (Fig. 3D, 3F, 4B, and 4D). This observation was further confirmed quantitatively by a dramatic decrease in the average optic density of MAP2 staining in deafferented dendrites (Fig. 5A and 5C). In the rostral portion of the nucleus, however, differences in MAP2 immunostaining between the deafferented and the intact dendrites were much less pronounced. Qualitatively, no difference was reliably detected in most cases across all survival times. Quantitative analysis of the average optic density demonstrated a small decrease of MAP2 staining in the deafferented dendrites in some cases with a survival times between 6h and 1 week (Fig. 5B and 5D).

Results of the percent difference calculations from the animals that received unilateral cochlea removal were analyzed by one-way ANOVA, followed by appropriate post hoc comparisons. Since there were no statistical differences between the ipsilateral and contralateral sides in terms of the amount of change in the deafferented vs. nondeafferented dendrite, data from the two sides of the brain were combined to increase the power. However, there were clear differences between the rostral (smaller) dendrites and the caudal (larger) dendrites. Hence these two data-sets were subjected to separate analyses. ANOVA on the data from caudal dendrites yielded a significant main effect ($F_{(5,25)} = 19.75$; $p<0.001$), and a highly significant trend toward increasing percent difference as a function of time following cochlea removal ($p< 0.001$; Post Test for Linear Trend). In addition, individual post hoc comparisons yielded highly significant differences between the control group and each of the other groups beginning at 3 hours after cochlea removal (3 hours, $p<0.01$; 6hr, 14 hr, 1 wk; $p<0.001$; Tukey's Multiple Comparison Test). As suggested by Figure 5, the analyses on the data from rostral NL dendrites did not yield results as clean as those from the caudal dendrites. Whether this was due to their smaller size and therefore greater percentage of error in the measurements, or differences in their biology can not be determined from our data. ANOVA yielded a significant main effect ($F_{(5,26)} = 3.40$; $p < 0.02$) indicating that there was a significant reduction of dendritic MAP2 immunoreactivity after cochlea removal on the deafferented dendrite. Post hoc Linear Trend Analysis also yielded a significant trend over time ($p < 0.01$) but only the 6hr group showed a reliable difference from controls ($p < 0.05$; Tukey's Multiple Comparison test).

XDCT transection resulted in decreases in MAP2 immunoreactivity in affected dendrites following a time course comparable to that in cases following cochlea removal (Fig. 6). Differences were first detected three hours after XDCT transection and presented as long as 14 hours later, the longest survival time examined. Figure 3G-H shows an example at 14 hour following XDCT transection. The ventral dendrites on both sides of the brain contained less

MAP2 immunoreactivity than the dorsal dendrites. Similar to the cases where one cochlea was ablated, this difference was most apparent in the caudal half of the nucleus. We did not perform statistical analyses on the data from animals with XDCT transection because the n's were too small. These experiments were included only to determine if the changes in MAP2 antibody reacted dendrites following this manipulation are similar to our previous data using a variety of other techniques for measuring dendritic change (Benes et al., 1977;Dietch and Rubel, 1984;1989;Sorensen and Rubel, 2006). Clearly the results are similar.

Discussion

Our results show that MAP2 immunoreactivity decreases rapidly and dramatically in deafferented dendrites of NL neurons, particularly in the caudal portion of the nucleus. We used two different methods to deprive one set of NL dendrites of its excitatory input: cochlea removal and XDCT transection. Both manipulations cause an immediate cessation of action potentials of excitatory NM afferents to affected NL dendrites (Born et al., 1991) and both appear to produce similar changes in MAP2 immunoreactivity in NL dendrites, as shown in the current study. Cochlea removal does not directly damage the NM axons that innervate NL dendrites and deafferentation-induced cell death in NM does not occur for 2 days (Born and Rubel, 1985). Therefore, the changes in MAP2 immunoreactivity in NL dendrites are likely to be a result of the elimination of presynaptic action potentials rather than frank degenerative changes or the release of degeneration-related cytokines from the presynaptic endings. However, we can not rule out release of degradative products from silenced endings.

We failed to detect comparable decreases in MAP2 immunoreactivity in rostral NL neurons. One possible explanation is that neurons in rostral NL have thinner dendrites and/or contain less MAP2 than caudal NL neurons. We observed lighter staining density of MAP2 in the rostral portion than in the caudal portion of the nucleus. Relative changes in MAP2 immunoreactivity may be obscured by low baseline levels of immunoreactivity. It is possible that there is just a smaller change in rostral NL compared to caudal NL. Dendritic MAP2 of NL neurons may be regulated to a varying degree, or by different mechanisms along the rostrocaudal axis. Further examination of MAP2 expression at an individual cell level may be necessary.

Decreases in the average density of MAP2 immunoreactivity may be partially due to the retraction of deafferented NL dendrites, which occurs as early as 1 hour following XDCT transection (Deitch and Rubel, 1984). Whether cochlea removal produces similar retraction of deafferented NL dendrites has not been studied within the survival time period examined in the current report. A previous study on the long-term regulation of deafferentation on dendritic structure reported a substantial preservation of the deafferented NL dendrites 4 weeks following cochlea removal (Rubel et al., 1981). Thus, it remains possible that the changes to dendritic structure and cytoskeleton following XDCT transection and cochlea removal are regulated via different mechanisms. On the other hand, this study also documented sprouting of axonal arbors from the intact NM to the 'deprived' dendritic region at these long survival times. Regardless, the current study revealed that following either manipulation, many individual dendritic branches in the deafferented dendritic domains appeared to contain less immunoreactivity than those in the intact dendritic domain. These observations suggest that a major contribution to the total decrease of MAP2 immunoreactivity comes from the loss of MAP2 immunostaining in remaining deafferented dendritic branches. This loss prior to structural changes of these dendrites suggests that changes in MAP2 may be one of the first steps in deprivation-induced dendritic atrophy. Given that dendritic retraction takes place as early as one hour following XDCT transection, yet distinct changes in MAP2 immunoreactivity were found three hours after the surgery, MAP2 may play a more significant role in the later

retraction of dendritic branches, than the initial disruption of the balance of growth and retraction (Sorensen and Rubel, 2006).

The decrease observed in MAP2 immunostaining could result from either the degradation of MAP2 protein or the alternation of its structure and/or binding properties, as previously suggested in deafferentation-induced MAP2 loss in NM somata (Kelley et al., 1997). Light microscopy used in the current report does not allow us to determine the nature of the changes in MAP2 immunoreactivity. Among all post-translational modifications of MAP2, phosphorylation is probably the most relevant to extracellular signals (for review, see Sánchez et al., 2000). MAP2 has been found to be a substrate for many protein kinases and phosphatases, including c-Jun N-terminal kinase1 (JNK1) and stathmin, whose phosphorylations of MAPs are important in defining neuronal dendritic structure (Björkblom et al., 2005; Ohkawa et al., 2007).

The decrease of MAP2 immunoreactivity, regardless of the cause, could be an indicator of changes in the normal function of MAP2. In support of this idea, changes in MAP2 immunoreactivity appear to be associated with changes in microtubules in deafferented dendrites. A quantitative analysis reported a 30–60% decrease in microtubules density in the initial portion of the ventral dendritic between 4–48 hours following XDCT transection (Deitch and Rubel, 1989). This time course is comparable to the changes in MAP2 immunoreactivity reported by the current study (see Fig. 5), giving rise to the assumption that MAP2 loss or alternation may interrupt its function on microtubule assembly and thus result in microtubule loss.

The rapid cellular events observed in NL dendrites following deprivation of afferent activity (overall dendritic retraction, interruption of the growth-retraction balance, decrease in MAP2 immunoreactivity, and microtubule loss) may be controlled by a single or separate mechanisms. Among a number of regulatory mechanisms controlling MAP2 function (see review, Sánchez et al., 2000), changes in calcium signaling, especially rises in intracellular calcium concentration ($[Ca^{2+}]_i$), have been most extensively studied following manipulations of synaptic inputs. Excessive glutamate receptor stimulation induced by physiological stimulation or exposure of glutamate or agonists of its receptors causes dendritic injury and/or MAP2 loss (Siman and Noszek, 1988; Bigot et al., 1991; Felipo et al., 1993; Arias et al., 1997; Faddis et al., 1997; Steward and Halpain, 1999; Swann et al., 2000; Vaillant et al., 2002). Recent studies in hippocampal slices further demonstrated that these changes are calcium-dependent (Hoskison and Shuttleworth, 2006; Hoskison et al., 2007). Here we demonstrated that loss of excitatory synaptic input, which might be assumed to cause a decrease in $[Ca^{2+}]_i$, also produces MAP2 loss or alternation. This observation is consistent with a previous report in the visual cortex following injections of tetrodotoxin into one eye (Hendry and Bhandari, 1992). To our knowledge, a direct link between decreases in $[Ca^{2+}]_i$ and MAP2 loss or alternation has not been reported. Another possibility is that the chronic decrease in synaptic activity could lead to an increase in $[Ca^{2+}]_i$. This possibility is supported by the dramatic increase of $[Ca^{2+}]_i$ in deafferented NM neurons (Zirpel et al., 1995; Zirpel and Rubel, 1996). In NL dendrites, this switch may result from a slow-down of the calcium efflux induced by downregulation of plasma membrane calcium ATPase isoform 2, one of the critical calcium efflux system, following deafferentation (Y. Wang, unpublished observations). Investigation on changes in NL dendritic $[Ca^{2+}]_i$ following deafferentation is required to confirm calcium signaling as one of the mechanisms by which deafferentation induces the observed change in NL dendritic MAP2, and previously described changes to NL dendrite structure.

Acknowledgments

The authors are proud to take part in this tribute to Kirsten Osen, a leader and model scientist in our field. The authors are grateful to Mr. MacKenzie A. Howard, Dr. Armin H. Seidl, Dr. Staci A. Sorensen, Ms. Kathryn M. Tabor, and Mr. Christopher K. Thompson for criticisms of the manuscript. The research was supported by NIDCD grants DC03829, DC04661 and DC00018.

Supported by National Institute on Deafness and Other Communication Disorders [DC-03829, DC00018, and DC-04661]

References

Arias C, Arrieta I, Massieu L, Tapia R. Neuronal damage and MAP2 changes induced by the glutamate transport inhibitor dihydrokainate and by kainate in rat hippocampus *in vivo*. Exp Brain Res 1997;116:467–476. [PubMed: 9372295]

Benes FM, Parks TN, Rubel EW. Rapid dendritic atrophy following deafferentation: an EM morphometric analysis. Brain Res 1977;122:1–13. [PubMed: 837214]

Bigot D, Matus A, Hunt SP. Reorganization of the cytoskeleton in rat neurons following stimulation with excitatory amino acids *in vitro*. Eur J Neurosci 1991;3:551–558. [PubMed: 12106487]

Björkblom B, Ostman N, Hongisto V, Komarovski V, Filén JJ, Nyman TA, Kallunki T, Courtney MJ, Coffey ET. Constitutively active cytoplasmic c-Jun N-terminal kinase 1 is a dominant regulator of dendritic architecture: role of microtubule-associated protein 2 as an effector. J Neurosci 2005;25:6350–6361. [PubMed: 16000625]

Born DE, Rubel EW. Afferent influences on brain stem auditory nuclei of the chicken: neuron number and size following cochlea removal. J Comp Neurol 1985;231:435–445. [PubMed: 3968247]

Born DE, Durham D, Rubel EW. Afferent influences on brainstem auditory nuclei of the chick: nucleus magnocellularis neuronal activity following cochlea removal. Brain Res 1991;557:37–47. [PubMed: 1747768]

Burger, RM.; Rubel, EW. Encoding of interaural timing for binaural hearing. In: Dallos, P.; Oertel, D., editors. The senses: a comprehensive reference. Elsevier; New York: 2007. p. 8-48.

Carr CE, Konishi M. Axonal delay lines for time measurement in the owl's brainstem. Proc Natl Acad Sci U S A 1988;85:8311–8315. [PubMed: 3186725]

Carr CE, Konishi M. A circuit for detection of interaural time differences in the brain stem of the barn owl. J Neurosci 1990;10:3227–3246. [PubMed: 2213141]

Deitch JS, Rubel EW. Afferent influences on brain stem auditory nuclei of the chicken: time course and specificity of dendritic atrophy following deafferentation. J Comp Neurol 1984;229:66–79. [PubMed: 6490976]

Deitch JS, Rubel EW. Rapid changes in ultrastructure during deafferentation-induced dendritic atrophy. J Comp Neurol 1989;281:234–258. [PubMed: 2708575]

Faddis BT, Hasbani MJ, Goldberg MP. Calpain activation contributes to dendritic remodeling after brief excitotoxic injury *in vitro*. J Neurosci 1997;17:951–959. [PubMed: 8994050]

Felipo V, Grau E, Minana MD, Grisolia S. Ammonium injection induces an N-methyl-D-aspartate receptor-mediated proteolysis of the microtubule-associated protein MAP-2. J Neurochem 1993;60:1626–1630. [PubMed: 8473887]

Folkerts MM, Berman RF, Muizelaar JP, Rafols JA. Disruption of MAP-2 immunostaining in rat hippocampus after traumatic brain injury. J Neurotrauma 1998;15:349–363. [PubMed: 9605349]

Harada A, Teng J, Takei Y, Oguchi K, Hirokawa N. MAP2 is required for dendrite elongation, PKA anchoring in dendrites, and proper PKA signal transduction. J Cell Biol 2002;158:541–549. [PubMed: 12163474]

Hendry SH, Bhandari MA. Neuronal organization and plasticity in adult monkey visual cortex: immunoreactivity for microtubule-associated protein 2. Vis Neurosci 1992;9:445–459. [PubMed: 1333277]

Hoskison MM, Shuttleworth CW. Microtubule disruption, not calpain-dependent loss of MAP2, contributes to enduring NMDA-induced dendritic dysfunction in acute hippocampal slices. Exp Neurol 2006;202:302–312. [PubMed: 16904106]

Hoskison MM, Yanagawa Y, Obata K, Shuttleworth CW. Calcium-dependent NMDA-induced dendritic injury and MAP2 loss in acute hippocampal slices. Neuroscience 2007;145:66–79. [PubMed: 17239543]

Joseph AW, Hyson RL. Coincidence detection by binaural neurons in the chick brain stem. J Neurophysiol 1993;69:1197–1211. [PubMed: 8492159]

Kelley MS, Lurie DI, Rubel EW. Rapid regulation of cytoskeletal proteins and their mRNAs following afferent deprivation in the avian cochlear nucleus. J Comp Neurol 1997;389:469–483. [PubMed: 9414007]

Kowalski RJ, Williams RC Jr. Microtubule-associated protein 2 alters the dynamic properties of microtubule assembly and disassembly. J Biol Chem 1993;268:9847–9855. [PubMed: 8486664]

Ohkawa N, Fujitani K, Tokunaga E, Furuya S, Inokuchi K. The microtubule destabilizer stathmin mediates the development of dendritic arbors in neuronal cells. J Cell Sci 2007;120(Pt 8):1447–1456. [PubMed: 17389683]

Overholt EM, Rubel EW, Hyson RL. A circuit for coding interaural time differences in the chick brainstem. J Neurosci 1992;12:1698–1708. [PubMed: 1578264]

Parks TN, Rubel EW. Organization and development of brain stem auditory nuclei of the chicken: organization of projections from n. magnocellularis to n. laminaris. J Comp Neurol 1975;164:435–448. [PubMed: 1206128]

Pettigrew LC, Holtz ML, Craddock SD, Minger SL, Hall N, Geddes JW. Microtubular proteolysis in focal cerebral ischemia. J Cereb Blood Flow Metab 1996;16:1189–1202. [PubMed: 8898691]

Rubel EW, Hyson RL, Durham D. Afferent Regulation of Neurons in the Brain Stem Auditory System. J Neurobiol 1990;21:169–196. [PubMed: 2181062]

Rubel, EW.; Parks, TN.; Zirpel, L. Assembling, Connecting, and Maintaining the Cochlear Nucleus. In: Parks, TN.; Rubel, EW.; Popper, AN.; Fay, RR., editors. Plasticity of the Auditory System, Series: Springer Handbook of Auditory Research. Vol. 23. Springer-Verlag; New York: 2004. p. 8-48.chapter 2

Rubel EW, Smith ZD, Steward O. Sprouting in the avian brainstem auditory pathway: dependence on dendritic integrity. J Comp Neurol 1981;202:397–414. [PubMed: 7298906]

Sánchez C, Diaz-Nido J, Avila J. Phosphorylation of microtubule-associated protein 2 (MAP2) and its relevance for the regulation of the neuronal cytoskeleton function. Prog Neurobiol 2000;61:133–168. [PubMed: 10704996]

Schwab M, Antonow-Schlorke I, Zwiener U, Bauer R. Brain-derived peptides reduce the size of cerebral infarction and loss of MAP2 immunoreactivity after focal ischemia in rats. J Neural Transm Suppl 1998;53:299–311. [PubMed: 9700666]

Serrano L, Avila J, Maccioni RB. Controlled proteolysis of tubulin by subtilisin: localization of the site for MAP2 interaction. Biochemistry 1984;23:4675–4681. [PubMed: 6388633]

Siman R, Noszek JC. Excitatory amino acids activate calpain I and induce structural protein breakdown in vivo. Neuron 1988;1:279–287. [PubMed: 2856162]

Smith ZDJ. Organization and development of brain stem auditory nuclei of the chicken: dendritic development in N. laminaris. J Comp Neurol 1981;203:309–333. [PubMed: 7320232]

Smith DJ, Rubel EW. Organization and development of brain stem auditory nuclei of the chicken: dendritic gradients in nucleus laminaris. J Comp Neurol 1979;186:213–239. [PubMed: 447882]

Sorensen SA, Rubel EW. The level and integrity of synaptic input regulates dendrite structure. J Neurosci 2006;26:1539–1550. [PubMed: 16452677]

Steward O, Halpain S. Lamina-specific synaptic activation causes domain-specific alterations in dendritic immunostaining for MAP2 and CAM kinase II. J Neurosci 1999;19:7834–7845. [PubMed: 10479686]

Swann JW, Al-Noori S, Jiang M, Lee CL. Spine loss and other dendritic abnormalities in epilepsy. Hippocampus 2000;10:617–625. [PubMed: 11075833]

Taft WC, Yang K, Dixon CE, Hayes RL. Microtubule-associated protein 2 levels decrease in hippocampus following traumatic brain injury. J Neurotrauma 1992;9:281–290. [PubMed: 1474611]

Vaillant AR, Zanassi P, Walsh GS, Aumont A, Alonso A, Miller FD. Signaling mechanisms underlying reversible, activity-dependent dendrite formation. Neuron 2002;34:985–998. [PubMed: 12086645]

Yamauchi PS, Flynn GC, Marsh RL, Purich DL. Reduction in microtubule dynamics in vitro by brain microtubule-associated proteins and by a microtubule-associated protein-2 second repeated sequence analogue. J Neurochem 1993;60:817–826. [PubMed: 7679726]

Zirpel L, Rubel EW. Eighth Nerve Activity Regulates the Intracellular Calcium Concentration of Cochlear Nucleus Neurons in the Embryonic Chick via a Metabotopic Glutamate Receptor. J Neurophysiol 1996;76:4127–4139. [PubMed: 8985906]

Zirpel L, Lachica EA, Lippe WR. Deafferentation increases the intracellular calcium of cochlear nucleus neurons in the embryonic chick. J Neurophysiol 1995;74:1355–1357. [PubMed: 7500157]

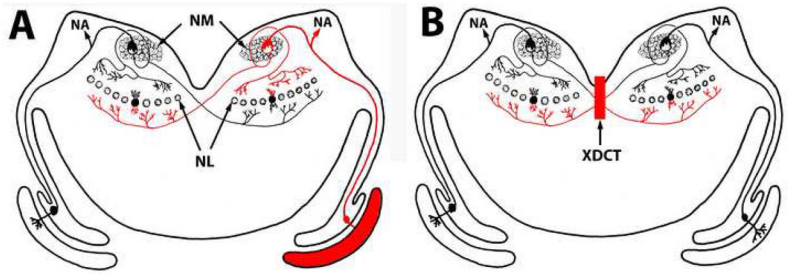

Figure 1.

Differential innervation of NL dendrites and the arrangement of the surgeries. Schematic drawings of the chick brainstem in the coronal plane illustrate the affected dendritic fields following unilateral cochlea removal (A) or XDCT transection (B). Red color indicates the surgical site for each manipulation and deafferented axons and dendrites influenced by each manipulation. Abbreviations: NL, nucleus laminaris; NM, nucleus magnocellularis; NA, nucleus angularis; XDCT, crossed dorsal cochlear tract.

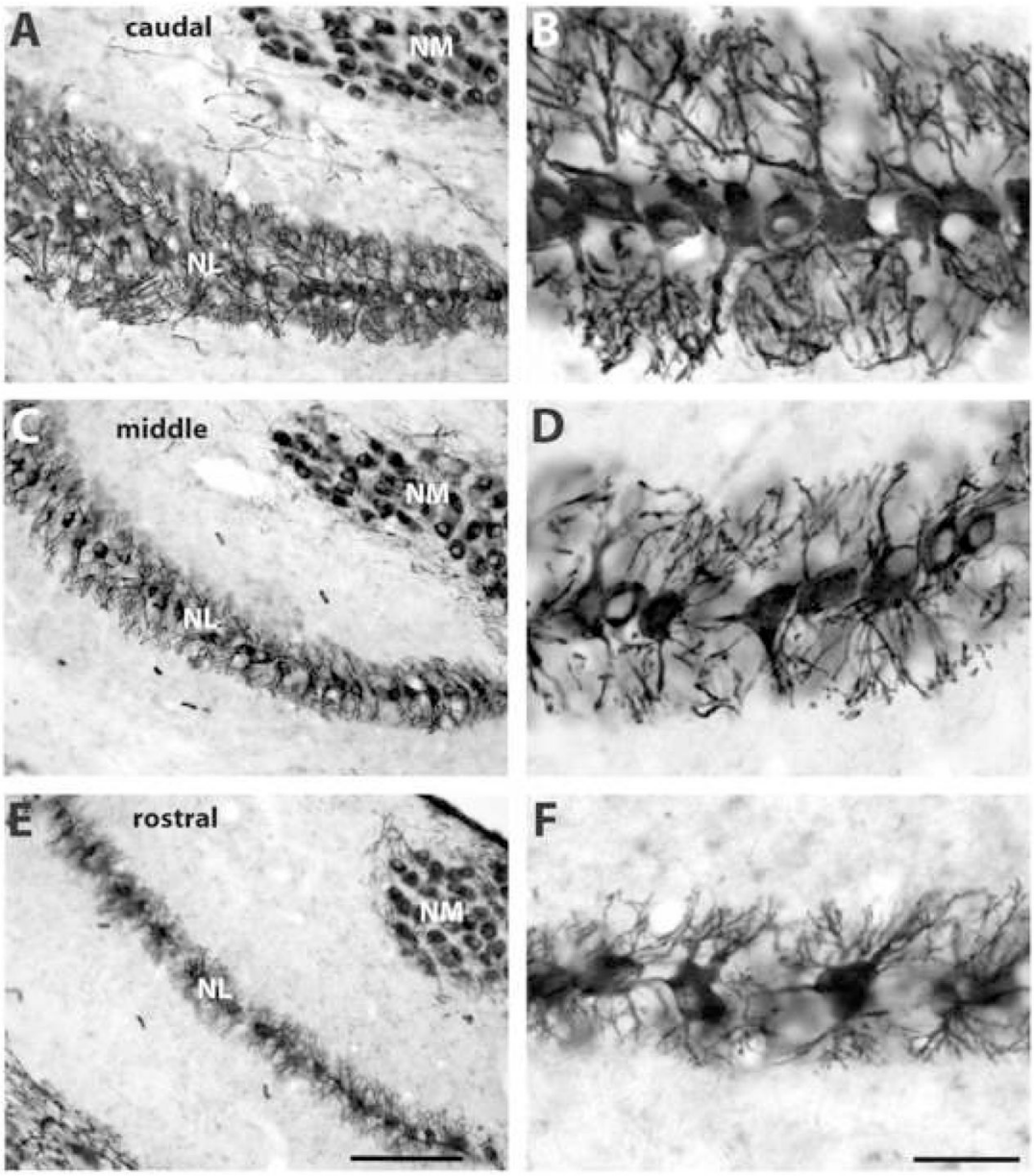

Figure 2.
MAP2 immunoreactivity in the normal chick NL at the caudal (A–B), middle (C–D), and rostral (E–F) levels. Sections were stained with peroxidase and intensified with nickel ammonium sulfate. Abbreviations see Figure 1. Scale bar = 100 μm in E (applies to A, C, E), 30 μm in F (applies to B, D, F).

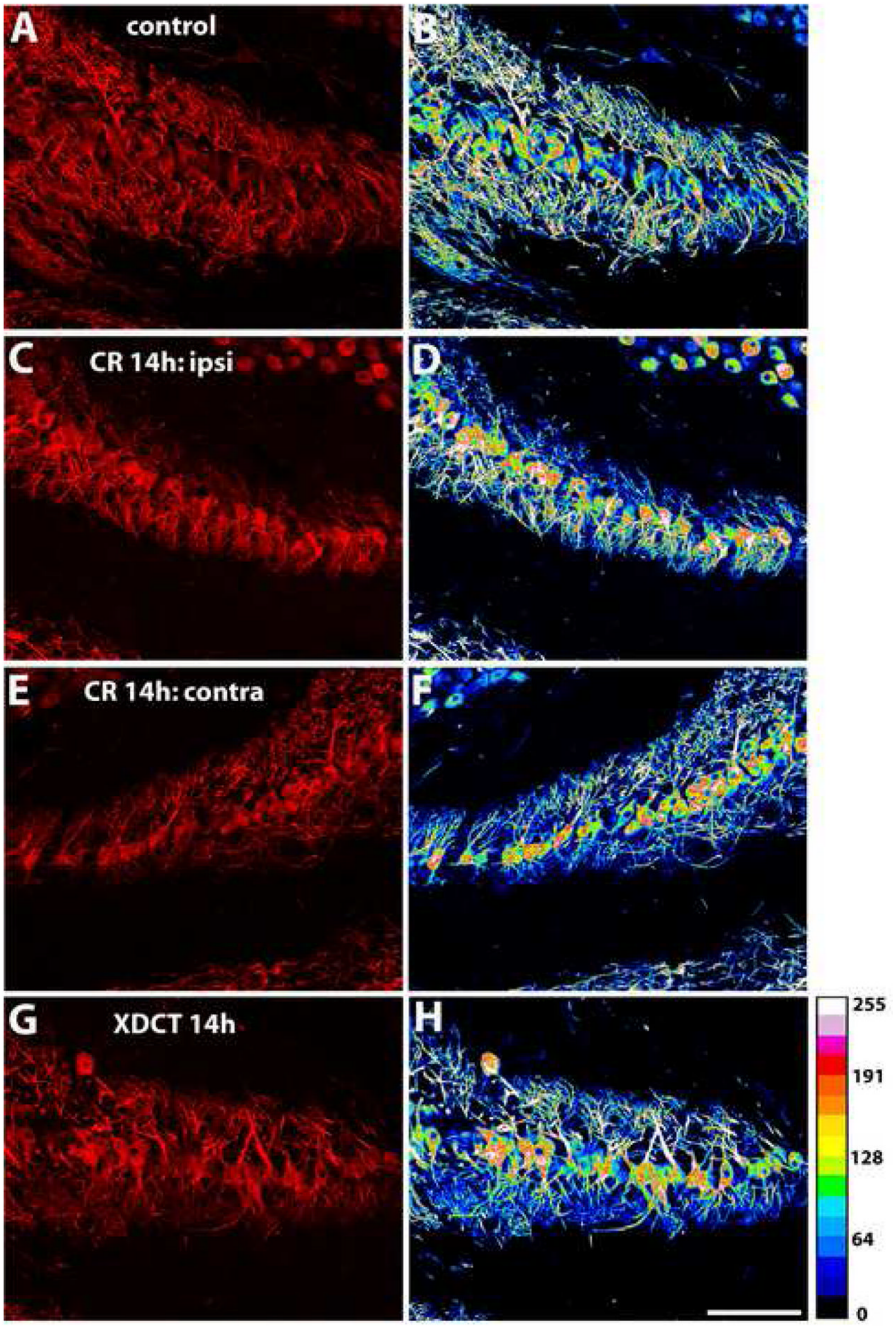

Figure 3.

MAP2 immunoreactivity in the caudal portion of NL before and 14 hours after cochlea removal or XDCT transection. **A–B:** In the normal NL, the staining density of MAP2 immunoreactivity is similar between the dorsal and ventral dendrites. **C–F:** MAP2 immunoreactivity in the ipsilateral (C-D) and the contralateral (E-F) NL at 14 hours following cochlea removal. Deafferented dorsal dendrites of the ipsilateral NL and ventral dendrites of the contralateral NL exhibited a distinct decrease in MAP2 immunoreactivity, as compared to the intact dendrites. **G–H:** MAP2 immunoreactivity in NL at 14 hours following XDCT transection. Deafferented ventral dendrites on both sides of the brain exhibited a distinct decrease in MAP2 immunoreactivity, as compared to the intact dorsal dendrites. A, C, E, and G are the confocal

photomicrographs. B, D, F, and H are the spectrums resulting from the corresponding photomicrographs using Image J software (version 1.38X; National Institutes of Health). These spectrum images use 16 colors to present different levels of the intensity in a photomicrograph. They demonstrate that deafferented dendritic domains contain less dendritic branches with high intensity of MAP2 immunoreactivity than the intact dendritic domain. Spectrum scale is presented on the lower right corner of the figure. Scale bar = 100 μm.

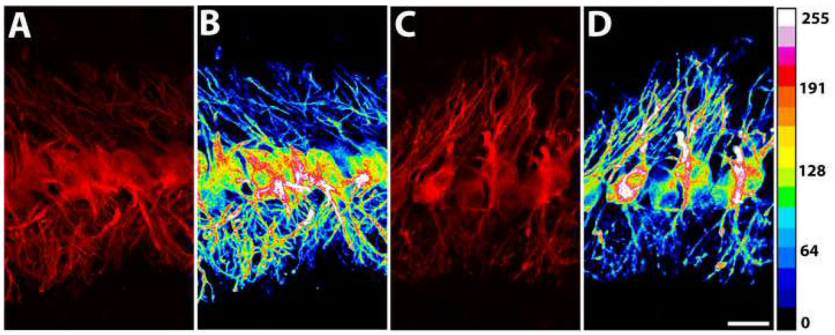

Figure 4.

High-magnification photomicrographs of MAP2 immunoreactivity in the caudal portion of the NL at 14 hours following cochlea removal. A and B are from the ipsilateral NL while C-D from the contralateral NL. B and D are the spectrum resulting from A and C, respectively. Spectrum scale is presented on the right side of the figure. Scale bar = 20 μm.

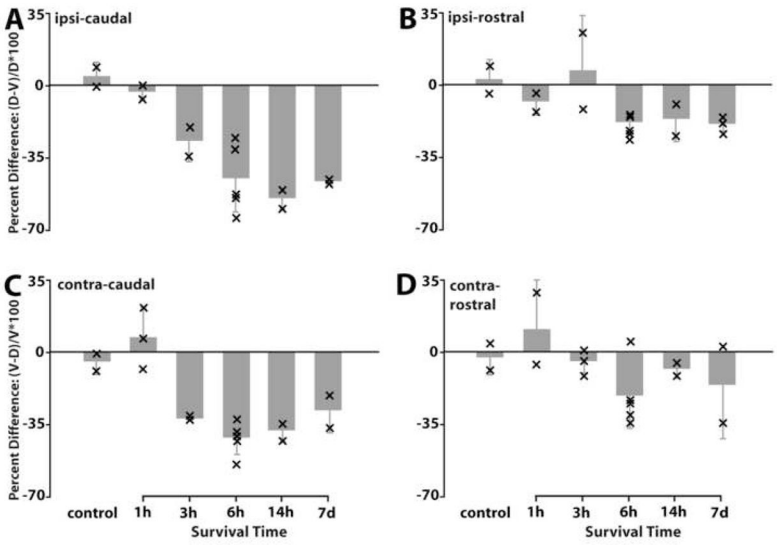

Figure 5.

Percent difference of the average optical density of MAP2 immunostaining between the dorsal and ventral neuropil domains as a function of the survival time following cochlea removal in the ipsilateral (**A–B**) and contralateral (**C–D**) NL. A and C are measured from the caudal NL while B and D from the rostral NL. The percent difference was calculated as the change in density of the deafferented (ventral in the contralateral side and dorsal in the ipsilateral side) neuropil domain relative to the intact (dorsal in the contralateral side and ventral in the ipsilateral side) domain. Bar graphs are the average percent difference from all animals in individual survival time group. Error bars are standard deviation. Each "×" indicates individual case data. The deafferented neuropil domains exhibited a notable decrease in MAP2 immunoreactivity compared to the intact domain in the caudal NL (A and C). This decrease was much less pronounced in the rostral NL (B and D).

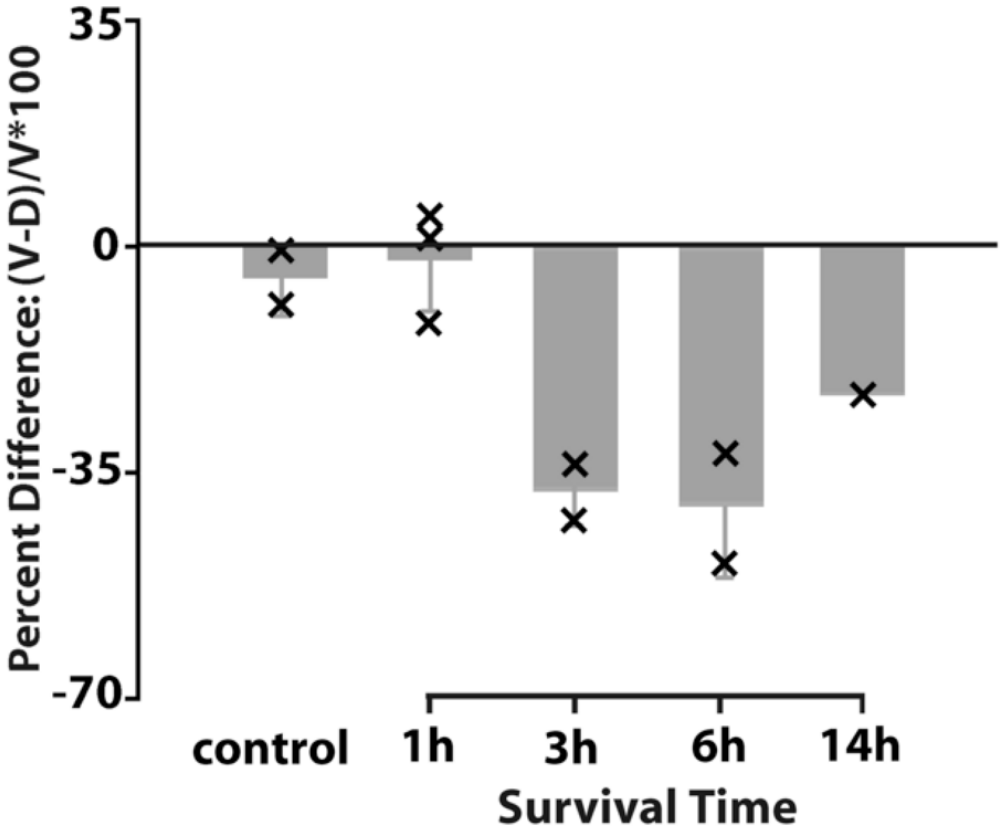

Figure 6.

Percent difference of the average optical density of MAP2 immunostaining between the dorsal and ventral neuropil domains as a function of the survival time following XDCT transection in the caudal NL. The Percent Difference was calculated as the change in density of the deafferented (ventral) neuropil domain relative to the intact (dorsal) domain. Data from the two sides of the brain were combined. Bar graphs are the average percent difference from all animals in individual survival time group. Error bars are standard deviation. Each "×" indicates individual case data. The deafferented ventral neuropil domains exhibited a notable decrease in MAP2 immunoreactivity compared to the intact dorsal domain.